https://doi.org/10.3311/PPci.41569

Periodica Polytechnica Civil Engineering, 70(1), pp. 123–132, 2026

Reliability Assessment of Local and Global Buckling Resistances for Reclaimed Welded Box-section Columns

Mohammad Radwan[1*], Balázs Kövesdi[1]

[1] Department of Structural Engineering, Faculty of Civil Engineering, Budapest University of Technology and Economics, Műegyetem rkp. 3., 1111 Budapest, Hungary
[*] Corresponding author, e-mail: mohammad.radwan@emk.bme.hu

Received: 10 July 2025, Accepted: 22 January 2026, Published online: 09 February 2026

Abstract

This study presents an enhanced method for evaluating the buckling resistance of reclaimed steel members by proposing modified local and global buckling formulas that align with the safety provisions of the Eurocode. Standard Eurocode formulas for local and global buckling resistance are insufficient for reclaimed members, as they do not account for the standard-based imperfection magnitudes and residual stress states commonly observed in reclaimed structures. To address this gap, new buckling resistance formulas were developed and calibrated through advanced geometrically and materially nonlinear analysis with imperfections (GMNIA). The reliability of the proposed formulas is evaluated in accordance with Annex D of EN 1990, enabling the derivation of appropriate partial safety factors for both local and global buckling modes. An additional safety factor is introduced to capture the interaction between these modes, ensuring a reliable safety assessment. The current study provides engineers with a practical method for evaluating the buckling capacity of reclaimed steel members, promoting safe and sustainable reuse in structural applications.

Keywords

partial factor, local buckling, flexural buckling, interaction buckling, reclaimed steel, equivalent imperfections

1 Introduction

Sustainability is reshaping modern engineering, presenting a growing challenge for engineers to extend the lifetime of steel structures. At the heart of this challenge lies the complex task of predicting the buckling capacity of steel-plated structures. A challenge made more complicated by the influence of residual stresses and inherent geometric imperfections. These effects are more pronounced in reclaimed structures, where in-service deterioration often results in greater imperfection magnitudes than current manufacturing standards permit [1–3]. Consequently, designing the reclaimed elements using the currently available local and global buckling resistance formulas available in Eurocode [4, 5] may not ensure safe design, as they do not adequately account for the elevated imperfections and the associated residual stresses formed during service. In a previous study [6], the authors investigated welded box-section columns and developed local and global imperfection factors α, which take into account the elevated values of imperfections and the resulting residual stresses during the formation of these imperfections. These imperfection factors can be used in the currently available buckling formulas in Eurocode [4, 5] to provide a more accurate estimation of the buckling capacity of reclaimed members. However, to use these improved buckling formulas in designing steel members, the EN 1990:2002 [7] requires performing a reliability study to consider the uncertainties in the proposed model and its basic variables. This reliability study yields the partial safety factor (γ_{M1}) that can be used to determine the design buckling capacity.

In this study, several reliability studies are performed to determine the partial safety factor (γ_{M1}) for the proposed local and global buckling formulas for square welded box-section columns. The proposed buckling capacities are compared against geometrically and materially nonlinear analysis with imperfections (GMNIA) that considers the increased imperfections and residual stresses. Furthermore, the interaction of local and global buckling capacity is also studied. This investigation will allow the designers to estimate the buckling capacity of reclaimed steel members more accurately.

Cite this article as: Radwan, M., Kövesdi, B. "Reliability Assessment of Local and Global Buckling Resistances for Reclaimed Welded Box-section Columns", Periodica Polytechnica Civil Engineering, 70(1), pp. 123–132, 2026. https://doi.org/10.3311/PPci.41569

2 Literature review

Statistical analysis based on probabilistic reliability theory is employed to evaluate the safety performance of the proposed resistance functions and to determine suitable partial safety factors. The assessment follows the Eurocode framework, utilizing the First-Order Reliability Method (FORM) to quantify the reliability level and ensure compliance with established safety criteria.

A set of procedures is available in Annex D of EN 1990:2002 [7] for obtaining the design values for a resistance function using statistical evaluation of experimental data. The procedure begins with formulating a design model for the theoretical resistance (r_t), as expressed in Eq. (1). This is followed by a comparative analysis between the theoretical resistance values ($r_{t,i}$), calculated using actual measured material and geometric properties, and the corresponding experimental results ($r_{e,i}$) obtained from experimental tests for each specimen. The least squares best-fit to the slope can be determined according to Eq. (2).

$$r_t = g_{rt}\left(X_i\right) \tag{1}$$

$$b = \frac{\sum r_{e,i} \cdot r_{t,i}}{\sum r_{t,i} \cdot r_{t,i}} \tag{2}$$

Each resistance pair ($r_{t,i}$, $r_{e,i}$) is used to calculate an error term δ_i, as depicted in Eq. (3).

$$\delta_i = \frac{r_{e,i}}{b \cdot r_{t,i}} \tag{3}$$

Eqs. (4) and (5) are used to calculate Δ_i and $\bar{\Delta}$ for a set of n experiments:

$$\Delta_i = \ln\left(\delta_i\right) \tag{4}$$

$$\bar{\Delta} = \frac{1}{n}\sum_{i=1}^{n}\Delta_i \tag{5}$$

The variance (s^2) and the coefficient of variation (V_δ) are calculated according to Eqs. (6) and (7), respectively.

$$s^2 = \frac{1}{n-1}\sum_{i=1}^{n}\left(\Delta_i - \bar{\Delta}\right)^2 \tag{6}$$

$$V_\delta = \sqrt{\left(\exp\left(s^2\right)-1\right.} \tag{7}$$

2.1 Uncertainties of the basic variables V_{Xi}

This study considers material strength (f_y), plate width (b_c), and thickness (t) as basic variables. The overall coefficient of variation (V_{rt}) combines the CoVs of these variables. EN 1990:2002 [7] offers different methods to calculate (V_{rt}) depending on the complexity of the resistance function. For independent variables, Eq. (8) applies to determine (V_{rt}).

$$V_{rt}^2 = \sum_{i=1}^{j} V_{Xi}^2 \tag{8}$$

2.2 Determination of partial safety factors γ_M and γ_M^*

For small values of V_{rt} and V_{Xi}, Eq. (9) can be used.

$$V_r^2 = V_{rt}^2 + V_\delta^2 \tag{9}$$

If the values of V_{rt} and V_{Xi} are not small, Eq. (10) must be used acc. to [8].

$$V_r^2 = \left(1+V_\delta^2\right)\left(1+V_{rt}^2\right)-1 \tag{10}$$

Equation (11) is used to calculate the partial safety factor (γ_{M1}), where r_k and r_d denote the characteristic and design resistances, defined by Eqs. (12) and (13), respectively.

$$\gamma_M = \frac{r_k}{r_d} \tag{11}$$

$$r_k = b \cdot g_{rt}\left(\underline{X}_M\right)\exp\begin{pmatrix} -k_\infty \alpha_{rt} Q_{rt} \\ -k_n \alpha_\delta Q_\delta - 0.5Q^2 \end{pmatrix} \tag{12}$$

$$r_d = b \cdot g_{rt}\left(\underline{X}_M\right)\exp\begin{pmatrix} -k_{d\infty} \alpha_{rt} Q_{rt} \\ -k_{d,n} \alpha_\delta Q_\delta - 0.5Q^2 \end{pmatrix} \tag{13}$$

$g_{rt}(X_M)$ is the theoretical resistance using mean values. Q_{rt}, Q_δ, and Q depend on the CoVs V_{rt}, V_δ, and V_r. Weighting factors α_{rt} and α_δ are as depicted in Eqs. D19.a–D19.b of/in EN 1990:2002 standard [7]. k_∞ is the 5% fractile for an infinite number of tests (1.64, Table D1 of/in EN 1990:2002 standard [7]) and the 1% fractile for design (3.04, Table D2 of/in EN 1990:2002 standard [7]) in EN 1990:2002 standard [7]. k_n and $k_{d,n}$ are fractile factors for unknown $V_{x,\text{unknown}}$ from Tables D1 and D2 of/in EN 1990:2002 standard [7].

The corrected safety factor (γ^*_M) is calculated using Eq. (14), with nominal values of the basic variables applied as per Eq. (15). This approach, presented by Taras and da Silva [9], da Silva et al. [10], Walport et al. [11], Heinisuo [12], Taras and Huemer [13] and Schillo et al. [8], generally provides a more accurate estimate of the necessary partial safety factor for the resistance model under analysis.

$$\gamma_M^* = \frac{\sum r_n \cdot r_n}{\sum r_n \cdot r_d} \tag{14}$$

$$r_n = g_{rt}\left(X_{nom}\right) \tag{15}$$

The target value for the corrected partial safety factor (γ^*_M) is 1.0 for buildings and 1.1 for bridges. For reclaimed members, a value of 1.15 is suggested [1].

An alternative method for calculating γ^*_M, used successfully in past studies [14–16], is given by Eq. (16). It uses Δk from Eq. (17), which adjusts for differences between nominal to mean, and characteristic difference in resistances. Δk is the ratio of the mean resistance with nominal inputs to the characteristic resistance.

$$\gamma^*_M = \Delta k \cdot \gamma_M \tag{16}$$

where:

$$\Delta k = \frac{r_{nom}}{r_k} = \frac{\exp\left(-2Q_{fy} - 0.5Q_{fy}^2\right)}{b \cdot \exp\left(-k_\infty Q - 0.5Q^2\right)} = \frac{0.867}{b \cdot \exp\left(-1.64Q - 0.5Q^2\right)} \tag{17}$$

and Q_{fy} is equal to 0.07 based on JCSS recommendations [17]. Several studies recommended a method by Afshan et al. [18], based on Annex D of EN 1990, that accounts for variable dependencies and overstrength. This reduces the uncertainty of the basic variables' uncertainty V_{rt}.

The dependency of the member resistance on the basic variables can be derived for each numerical simulation using different exponents *c*, *d*, and *e* that are applied to the basic variables, as depicted in Eqs. (18)-(20). The $N_{1.05fy}$, $N_{1.05t}$, and $N_{1.05b}$ represent the buckling resistances obtained from numerical analyses with yield stress f_y, thickness *t*, and width *b* multiplied by 1.05, respectively. The N_{fy}, N_t, and N_b are the obtained buckling resistances from the unmodified values of f_y, *t*, and *b*.

$$c = \frac{\ln\left(\frac{N_{1.05f_y}}{N_{f_y}}\right)}{\ln\left(\frac{1.05f_y}{f_y}\right)} \tag{18}$$

$$d = \frac{\ln\left(\frac{N_{1.05t}}{N_t}\right)}{\ln\left(\frac{1.05t}{t}\right)} \tag{19}$$

$$e = \frac{\ln\left(\frac{N_{1.05b}}{N_b}\right)}{\ln\left(\frac{1.05b}{b}\right)} \tag{20}$$

The coefficient of variation (V_{rt}) in this method is determined according to Eq. (21) [18].

$$V_{rt} = \sqrt{\left(cV_{fy}\right)^2 + \left(dV_t\right)^2 + \left(eV_b\right)^2} \tag{21}$$

This method uses overstrength factors ($f_{y,\text{mean}}/f_{y,\text{nom}}$) to produce a more reliable corrected partial safety factor γ^*_M. The overstrength factors are listed in Table 1.

Following the recommendations of [18] and [19], the following modifications can be adopted to account for the dependent variables and the overstrength factors, where the is determined according to Eq. (22).

$$\gamma^*_M = \frac{\sum r_{n,i}^2}{\sum r_{n,i} \cdot r'_{d,i}}, \tag{22}$$

where

$$r'_{d,i} = r_d \exp\left(c \cdot \ln\left(\frac{f_{y,mean}}{f_{y,nom}}\right)\right).$$

3 The developed numerical model

A numerical model is developed in Ansys [20] using four-node thin shell elements (SHELL181), as shown in Fig. 1. Loading and boundary conditions are applied via two master nodes located at the centers of the end cross-sections. Coupling constraints are used to connect the master nodes to all node locations on the end cross-sections, ensuring coupling in all six degrees of freedom. For the first master node, constraints are applied to prevent translation in the global directions (UX, UY, UZ) and rotation about the longitudinal axis (RZ), thereby simulating a pinned boundary condition and preventing the member from rotating freely along its axis. Meanwhile, the second master node is constrained against translation in the (UX, UY) directions and against rotation about (RZ), allowing deformation in the UZ direction.

A mesh sensitivity analysis is performed to identify an optimal mesh size that ensures accurate results while

Table 1 Overstrength factors for different steel types [8]

Grade	235	355	460
$f_{y,\text{mean}}/f_{y,\text{nom}}$	1.25	1.2	1.15

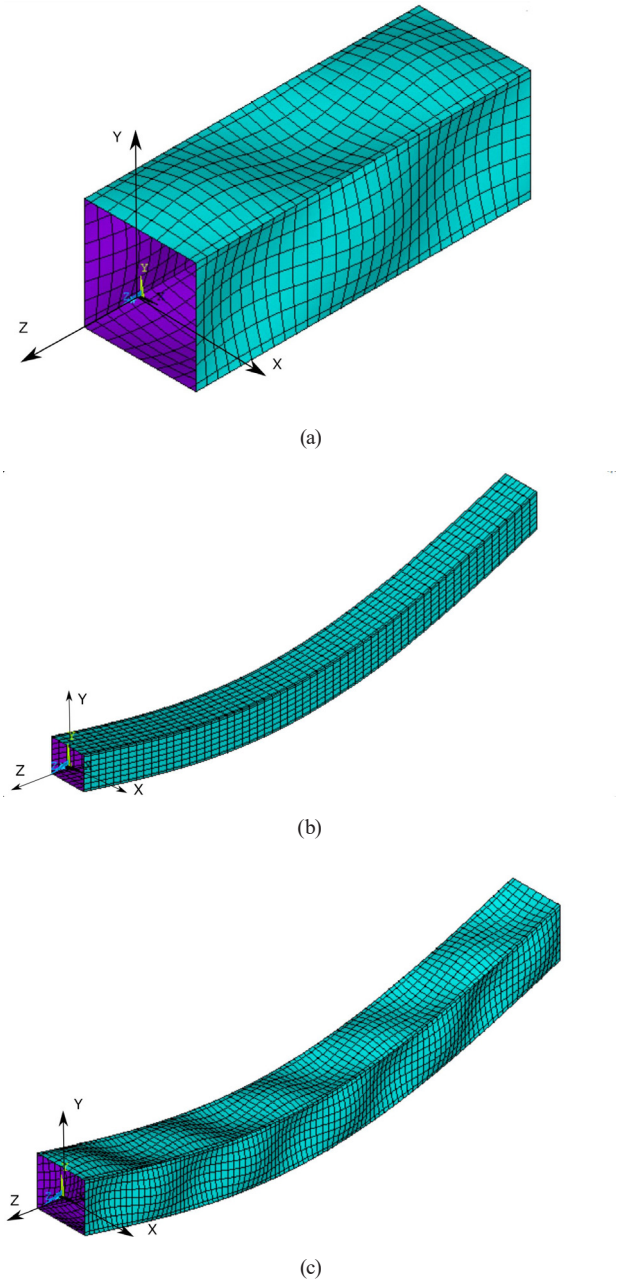

Fig. 1 (a) Local, (b) global, and (c) interaction definitions of imperfections for box sections [21]

minimizing computational demand. This analysis is conducted for box-section members with the smallest and largest plate widths considered in the study, capturing a representative range of geometries. The results indicate that a mesh size equal to $b/20$, where b is the plate width, offers a reliable prediction of buckling resistance with acceptable computational efficiency. This mesh size adequately captures local and global buckling modes without significantly increasing the solution time. Further details on the applied material model and mesh sensitivity analysis are available in [22, 23].

The residual stress model illustrated in Fig. 2 is adopted in this study, as recommended by the ECCS (European Convention for Constructional Steelworks) [24] and prEN 1993-1-14 [25]. Positive values denote tensile residual stresses, while negative values indicate compressive stresses. This residual stress model is applied in conjunction with the non-amplified imperfections considered in the analysis.

The effect of amplified imperfections and the stresses that develop during their formation is evaluated by considering two types of imperfections: (i) non-amplified imperfections, representing the inherent geometric imperfections present before loading, and (ii) displacements of the same shape as the non-amplified imperfections, simulating those that develop during the service life of the member. These displacements will cause the formation of the amplified imperfections and stresses in the member.

The modelling of non-amplified local and global imperfections is achieved by manually altering the idealized geometry of the finite element model. This is done by adjusting the positions of selected nodes to introduce imperfection amplitudes, either added or subtracted from the original geometry, to take into account the effect of initial geometric imperfections typically observed in real structural members. This approach enables the simulation of realistic buckling behavior by incorporating imperfections prior to loading. A detailed description of the modelling procedure and its validation is provided in the authors' earlier work [21]. Local imperfections are modelled using integer multiples of half sine waves, determined based on the L/b ratio, where L is the column length and b is the plate width of the box section. These imperfections are introduced along each plate in the longitudinal direction, with alternating amplitudes on adjacent

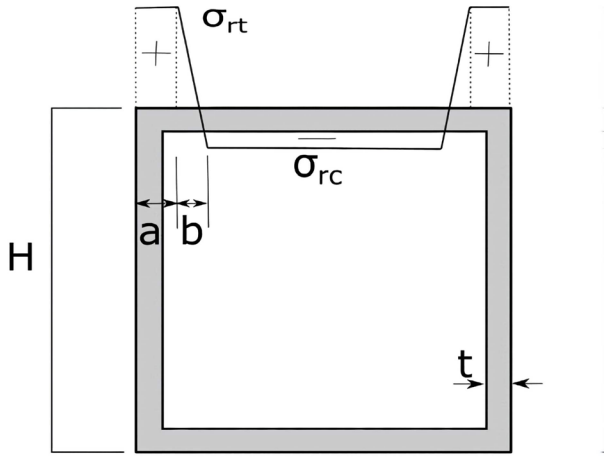

Fig. 2 Residual stress model for welded box section columns [24, 25]

plates to reflect first eigen buckling mode, as shown in Fig. 1(a). Global imperfections, on the other hand, are represented by a continuous half sine wave extending along the entire length of the column, as illustrated in Fig. 1(b). For cases involving interaction buckling, both local and global imperfections are simultaneously applied to the model, as depicted in Fig. 1(c). This modelling strategy has been validated through various studies, which confirm that it provides a consistent and reliable estimation of buckling resistance in structural members [26]. Amplified imperfections are introduced as displacements distributed along the column plates. It is essential to note that this method relies on the assumption that the imperfections and residual stresses generated during service can be approximated by these displacements. The analysis follows a three-step procedure designed to approximately simulate the key stages a reclaimed column experiences throughout its service life. In the first step, the column model is analyzed with non-amplified imperfections and residual stresses to represent the inherent imperfections that exist prior to service loading. In the second step, displacements are applied to impose amplified imperfections, simulating the additional deformations and stresses that may develop during the column's previous service period. In the final step, these displacements are removed while retaining the induced stresses, and a compressive load is applied at the master node to evaluate the column's buckling behavior under its current condition. After each step, the stress state and geometry are captured using the `INISTATE` and `UPGEOM` commands to ensure continuity and accuracy between analysis stages. During the first two stages, the loads are applied at their designated magnitudes, whereas in the third stage, the analysis is terminated when numerical convergence is no longer attainable. It is important to note that the imposed displacements follow the same shape and sign as the initial non-amplified imperfections, effectively amplifying their magnitudes. In the case of interaction buckling, local and global imperfection shapes are superimposed and applied simultaneously through a unified displacement loading pattern. The validation of this numerical model has been comprehensively addressed in the authors' previous work on welded box section columns [21], where numerical results were benchmarked against experimental data. The validated model showed excellent agreement, yielding a mean buckling capacity ratio of 1.0 and a coefficient of variation (CoV) of 0.06, confirming its reliability in predicting structural performance.

4 Effect of imperfection amplitude on buckling capacity

4.1 Local buckling resistance

Short columns with a length-to-width ratio of three ($L = 3b$) are examined to evaluate their local buckling resistance. In a previous study [23], local imperfections were calibrated to match the Annex B buckling curve of EN 1993-1-5 [5]; these non-amplified imperfections yield a baseline numerical resistance R_{en_base}. These imperfections are amplified by amplification ratios (r_{amp}) of 1.2, 1.5, 2, and 3.0 to obtain the amplified imperfections and to produce the amplified buckling resistance R_{en_amp}. To illustrate the influence of imperfection amplification, Fig. 3 presents load-deformation curves for three specimens having a local slenderness ratio of ($\bar{\lambda}_p = 1.35$). It shows a curve obtained with non-amplified imperfections ("No-amp") is compared against that with amplified imperfections of a value of $r_{amp} = 3.0$. Amplified imperfections are introduced using two approaches: (i) by directly modifying node positions ("Node-amp"), as done in the authors' earlier work [22], and (ii) by applying displacement loads ("Disp-amp"). Fig. 3 illustrates the Von Mises stress distribution for the "Disp-amp" method at key points along the load-deformation curve. The first image shows the stress state at the onset of the buckling analysis. Unlike the Node-amp method, which assumes imperfections develop without inducing additional stresses, the Disp-amp method captures both the amplified imperfections and the stresses generated during their formation.

Fig. 4(a) shows the results of the performed numerical study, where the y-axis shows the normalized amplified capacity to the base capacity for a wide range of local slenderness. It can be seen that the greatest reduction occurs for ($r_{amp} = 3.0$). The non-homogeneous trend originates from residual stresses carried over from the previous analysis, induced by the displacements applied as imperfections. These stresses contribute to greater instability, particularly

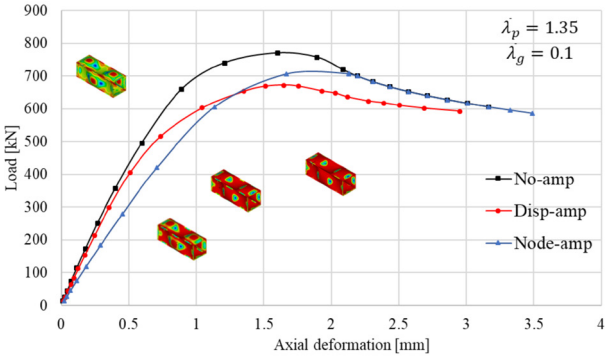

Fig. 3 Load-deformation curves for the studied methods

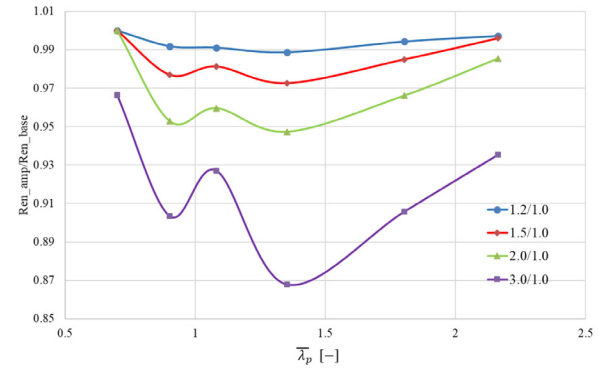

(a)

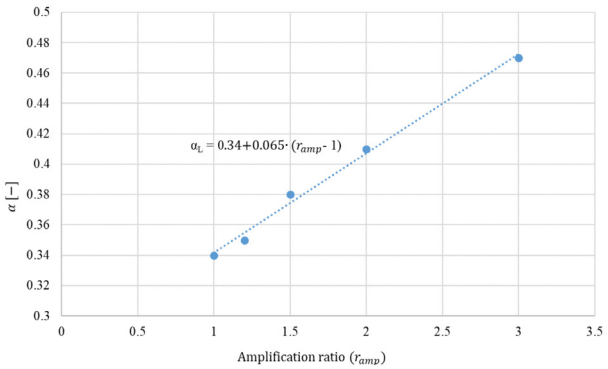

(b)

Fig. 4 (a) Normalised numerical results for pure local buckling analysis of box section columns using displacement load imperfection method (Disp-amp). (b) The relationship between the amplification ratio (ramp) and the α value in Eq. (23) [16].

in the medium slenderness range. The results of the imperfection calibration process against the GMNIA are shown in Fig. 4(b), where x-axis shows the amplification factor (r_{amp}), while y-axis shows the local imperfection factor α_L. The calibration of α_L was carried out by adjusting its value to minimize the discrepancy between the theoretical and numerical results. The straight-line behavior arises from the nature of the Eurocode buckling curve, whose general trend slightly differs from the obtained numerical results. It means, the buckling curve available in Annex B of EN 1993-1-5 [5] can be modified to include the effect of amplified imperfection, as depicted in Eqs. (23) and (24). The reliability study will be performed to estimate a partial safety factor for this formula.

$$\alpha_L = 0.34 + 0.065 \cdot \left(r_{amp} - 1\right) \tag{23}$$

$$\rho = \frac{1}{\phi_P + \sqrt{\phi_P^2 - \overline{\lambda}_p^2}}$$
$$\phi_p = \frac{1}{2}\left(1 + \left(0.34 + 0.065 \cdot (r_{amp} - 1)\right)\left(\overline{\lambda}_p - 0.7\right) + \overline{\lambda}_p\right) \tag{24}$$

4.2 Global buckling resistance

Pure global buckling behavior is studied using the geometric configurations reported in [6]. The non-amplified global imperfection is introduced by adjusting the nodal positions of the column geometry. In contrast, the amplified imperfection is applied as a displacement load distributed along the full column length. A global imperfection amplitude of $L/1000$ is used, in combination with the residual stress distribution also defined in [6], to represent realistic initial conditions. The amplified imperfections are defined as described previously. Fig. 5 shows the normalized resistance obtained using GMNIA and the calibrated imperfection factors $\boldsymbol{\alpha_g}$ for global buckling. Eqs. (25)-(26) represents the modified buckling curve for global buckling.

$$\alpha_g = 0.34 + 0.17 \cdot \left(r_{amp} - 1\right) \tag{25}$$

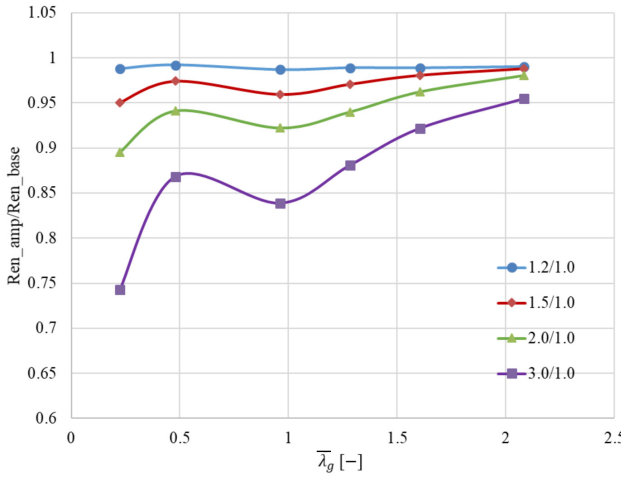

(a)

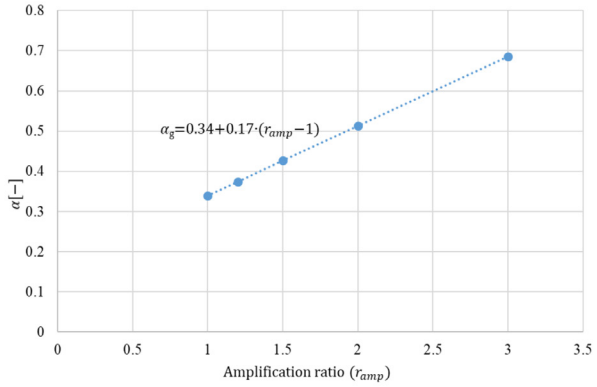

(b)

Fig. 5 (a) Normalised numerical results for pure global buckling analysis of box section columns using the displacement load imperfection method (Disp-amp). (b) Correlation between the amplification ratio (r_{amp}) and the α imperfection factor in Eq. (6.49) [12] using the displacement load imperfection method.

$$\chi = \frac{1}{\phi + \sqrt{\phi^2 - \bar{\lambda}_g^2}}$$
$$\phi = 0.5[1 + \alpha_g \left(\bar{\lambda}_g - 0.2\right) + \bar{\lambda}_g{}^2 \tag{26}$$

4.3 Interaction buckling resistance

For columns exhibit both local and global slenderness, require the application of imperfections in both modes. Global imperfections are set to *L*/1000, while local imperfections follow the Annex B calibration, with a peak value of *b*/125 [23]. These imperfections, combined with residual stresses, are treated as non-amplified imperfections. A similar procedure, as described earlier, is adopted to apply both local and global amplified imperfections using the amplification factors shown earlier. Both local and global imperfections are applied simultaneously using the same amplification factors. The resulting numerical resistances are then compared to the theoretical interaction buckling resistances, which are determined using the calibrated formulas for local and global buckling Eqs. (23)-(26).

5 Reliability analysis

To ensure that the calibrated formulas for local and global buckling satisfy the safety requirements of the Eurocode, the method "design assisted by testing" available in Annex D of EN 1990:2002 [7] is used. The details of the applied method are described in Section 2. In this study, the resistance obtained using GMNI analysis is considered as the benchmark resistance (r_e), and the resistance obtained using the developed formulas is considered as the theoretical resistance (r_t). The theoretical resistance for local buckling is defined by Eqs. (23)-(24), while for global buckling is defined by Eqs. (25)-(26). For interaction buckling, the product of these two equations is used. Two methods are applied and compared to determine the partial safety factors: (i) the first uses the normalized numerical-to-theoretical resistances, (ii) while the second one compares the non-normalized resistances. The first method demonstrates the ability of the proposed formulas to capture the trend observed in the numerical results, whereas the second method evaluates their accuracy in estimating the buckling resistance relative to the numerical results. Table 2 shows the coefficient of variations for each parameter considered in the uncertainty of the model.

5.1 First method: normalized resistances

In this method, the normalized resistances are utilized, as shown in Eq. (27), where the normalized numerical resistance is divided by the normalized resistance obtained by the local and global buckling formulas.

Table 2 Coefficient of variations for each parameter

Parameter	CoV
Plate thickness V_t	0.05
Plate width V_b	0.005
Yield strength V_{fy}	0.07

$$\text{ratio} = \frac{\left(\frac{R_{amp}}{R_{base}}\right)_{\text{Numerical}}}{\left(\frac{R_{amp}}{R_{base}}\right)_{\text{Formula}}} \tag{27}$$

Table 3 shows a summary of the performed reliability assessment, where the mean value correction *b* is calculated according to Eq. (2), while the coefficient of variations (V_δ) according to Eq. (7). The overall coefficient of variations (V_{rt}), which accounts for the variability of the basic input parameters is calculated according to Eq. (8). The total coefficient of variations (V_r) is calculated according to Eq. (10). The partial safety factor (γ_{M1}) is calculated according to Eq. (11) and the corrected partial safety that incorporates nominal input parameters is calculated according to Eq. (16). As shown in Table 3, the mean correct factor (*b*) is larger than 1.00, and the coefficient of variations is relatively small for all types of buckling, indicating reliable fit. However, the method in EN 1990:2002 [7] requires the determination of the partial safety factor, which includes the effect of the uncertainty of the basic variables, shown in Table 2. The obtained partial safety factors (γ_{M1}) are around 1.14 for local buckling, 1.16 for global buckling, and 1.18 for interaction buckling. To account for the effect of nominal values and the overstrength ratio, which various authors have shown to impact the estimation of the partial safety factor [9–11]. The corrected partial safety factor (γ^*_{M1}) is calculated using the Δk method outlined in Section 2. The obtained partial safety factors (γ^*_{M1}) are around 1.13 for local buckling, 1.15 for global buckling, and 1.17 for interaction buckling. It can be seen that a small reduction has been achieved. However, the obtained corrected partial safety factors are still relatively large, mainly due to the uncertainty of the

Table 3 Statistical evaluation of the studied methods (Δk method)

Type	b	V_δ	V_{rt}	V_r	γ_{M1}	γ^*_{M1}
Local	1.00	0.010	0.086	0.087	1.14	1.13
Global	1.01	0.033	0.086	0.092	1.16	1.15
Interaction	1.02	0.060	0.086	0.105	1.18	1.17

basic variables (V_{rt}), which, as shown in Table 3, is larger than (V_δ). In a previous study conducted by the authors on amplified imperfections, which did not account for the effect of induced stresses [22], comparable values were found for V_r and γ^*_{M1}. However, slightly higher values of V_r are observed here due to the inclusion of stresses induced during imperfection formation.

To provide a better estimate of the partial safety factors for each buckling mode, a more comprehensive method is used to take into account the sensitivity of each analyzed model to each basic variable. It takes into account the interdependency of the basic variables, aiming to more realistically represent actual behavior. This method, originally developed by Afshan et al. [18], is explained in detail in Section 2. In this method, the V_{rt} is calculated for each test according to Eq. (21), where a modification factor is applied to the coefficient of variation of each basic variable. The modification factors (*c*, *d*, and *e*) utilized in this study are depicted in Eqs. (18)-(20). These factors are determined for each test specifically, utilizing non-normalized resistances. Additionally, this method incorporates the effect of the nominal values of the yield strength and the overstrength ratio. Several researchers utilized this method to estimate partial safety factors for buckling problems [11, 27–32]. The results of the reliability study performed using this method are presented in Table 4. It can be observed that the resulting partial safety factors are smaller than those obtained using the Δk method.

5.2 Second method: non-normalized resistances

While the previous method shows the general ability of the provided formulas to capture the trend observed by the numerical model, the current method shows the consistency in estimating the buckling resistance. This method compares the non-normalized resistances, where the reliability assessment is based on the ratio depicted in Eq. (28). The results of the performed study are shown in Fig. 6, where the x-axis shows the theoretical resistance (r_t), and the y-axis shows the benchmark resistance (r_e). The comparison shows that the developed formulas provide a generally robust estimation of the buckling resistance. A summary of the performed analysis is shown in Table 5. It can be observed that the mean correction value (*b*) is equal to or larger than 1.0, and the coefficient of variation is relatively small ($V_\delta < 0.02$) for all types of buckling. This suggests

Table 4 Statistical evaluation of the studied methods [18]

Type	b	V_δ	V_{rt}	V_r	γ^*_{M1}
Local	1.00	0.010	0.07	0.071	1.00
Global	1.01	0.033	0.08	0.087	1.00
Interaction	1.02	0.060	0.09	0.104	1.05

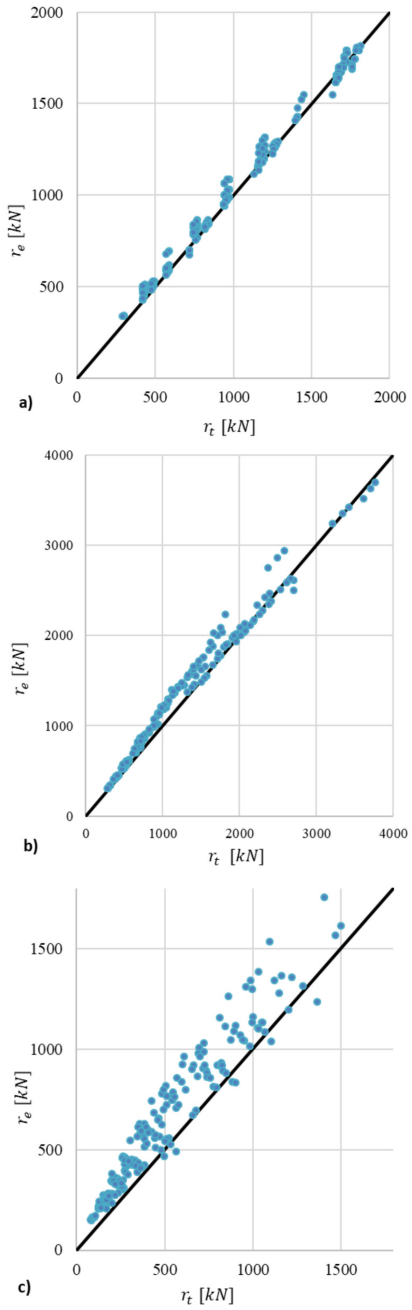

Fig. 6 Theoretical buckling capacity vs the benchmark (numerical) buckling capacity for (a) local buckling, (b) global buckling and (c) interaction buckling

Table 5 Statistical evaluation of the studied methods

Type	b	V_δ	V_{rt}	V_r	γ^*_{M1}
Local	1.00	0.00	0.07	0.10	0.99
Global*	1.04	0.01	0.08	0.12	1.01
Interaction*	1.20	0.02	0.09	0.19	1.15

*Limited: $\bar{\lambda}_g > 0.4$ and $r_{amp} \leq 2.0$

a generally safe estimation of the buckling resistance. The corrected partial safety factor, calculated according to Eq. (22), is equal to 1.0 for local buckling, 1.01 for global buckling, and 1.15 for interaction buckling. It is worth mentioning that a larger discrepancy exists for global and interaction buckling behavior compared to the local buckling. This is mainly because the numerical simulations capture complex behaviors that are not fully represented by the simplified Eurocode buckling formulas. However, several researchers showed that for reclaimed members, a value of $\gamma_{M1} = 1.15$ can be used [1]. It should be noted that the reliability study is restricted to $\bar{\lambda}_g > 0.4$ and $r_{amp} \leq 2.0$, since the buckling curves were unable to accurately reflect the numerical model behavior outside these limits.

$$\text{ratio} = \frac{\left(R_{amp}\right)_{\text{Numerical}}}{\left(R_{amp}\right)_{\text{Formula}}} \tag{28}$$

6 Conclusions

This study presented a reliability assessment of reclaimed welded box-section steel members prone to local, global, and interaction buckling. The study mainly focused on investigating the reliability of newly developed local and global buckling formulas that take into account the effect of amplified imperfections in reclaimed members and the generated residual stresses during the formation of the imperfection during the service time of the members [6]. The developed formulas were calibrated against GMNI analyses, which take these effects into account. The method available in Annex D of EN 1990 is used to evaluate the reliability of the proposed formulas. The results demonstrated consistent mean correction factors ($b \geq 1.0$) and low coefficients of variation ($V_\delta < 0.02$), indicating accurate estimations of buckling resistances. Corrected partial safety factors were proposed for local, global, and interaction buckling modes. The findings demonstrate that the current Eurocode resistance formulas may not be directly applicable to reclaimed members due to elevated imperfection magnitudes that cause a large reduction in capacity. When designing reclaimed structural members, the actual geometric imperfections should be measured, and the characteristic capacity evaluated using the proposed buckling curves. The design resistance is then obtained by applying the appropriate partial safety factors to ensure safety requirements. The modified design approach, supported by calibrated safety factors, provides a practical and safe framework for the structural assessment and reuse of existing steel members, contributing to sustainable engineering practices.

Acknowledgment

The presented research program has been financially supported by the Grant MTA-BME Lendület LP2021-06/2021 "Theory of new generation steel bridges" program of the Hungarian Academy of Sciences and Stipendium Hungaricum Scholarship. Both grants are gratefully acknowledged.

References

[1] Girão-Coelho, A., Pimentel, R., Ungureanu, V., Hradil, P., Kesti, J. "European recommendations for reuse of steel products in single-storey buildings", European Convention for Constructional Steelwork (ECCS), 2020. ISBN 978-92-9147-170-6

[2] Korol, R. M., Thimmhardy, E. G., Cheung, M. S. "Field investigation of out-of-plane deviations for steel box girder bridges", Canadian Journal of Civil Engineering, 11(3), pp. 377–386, 1984. https://doi.org/10.1139/l84-058

[3] Thimmhardy, E. G., Korol, R. M. "Geometric imperfections and tolerances for steel box girder bridges", Canadian Journal of Civil Engineering, 15(3), pp. 437–442, 1988. https://doi.org/10.1139/l88-059

[4] European Committee for Standardization "EN 1993-1-1:2005 Eurocode 3: Design of steel structures - Part 1-1: General rules and rules for buildings", CEN, Brussels, Belgium, 2005.

[5] European Committee for Standardization "EN 1993-1-5:2006 Eurocode 3: Design of steel structures, Part 1.5: Plated structural elements", CEN, Brussels, Belgium, 2006.

[6] Radwan, M., Kövesdi, B. "Improved buckling reduction factors for reclaimed steel members considering imperfections and stresses", Journal of Constructional Steel Research, 233, 109679, 2025. https://doi.org/10.1016/j.jcsr.2025.109679

[7] European Committee for Standardization "EN1990:2002 Eurocode–Basis of structural design", CEN, Brussels, Belgium, 2002.

[8] Schillo, N. "Local and global buckling of box columns made of high strength steel", Dissertation, Rheinisch-Westfälische Technische Hochschule Aachen, 2017. https://doi.org/10.18154/RWTH-2017-07053

[9] Taras, A., da Silva, L. S. "European Recommendations for the Safety Assessment of Stability Design Rules for Steel Structures", ECCS Technical Committee, Brussels, Belgium, ECCS–TC8-2012–06, 2012.

[10] Simões da Silva, L., Tankova, T., Marques, L., Rebelo, C. "Comparative Assessment of semi-probablistic methodologies for the safety assessment of stability design rules in the framework of annex D of EN 1990", ECCS Technical Committee, Coimbra, Portugal, ECCS–TC8-2013–11–024, 2013.

[11] Walport, F., Gardner, L., Nethercot, D. A. "Equivalent bow imperfections for use in design by second order inelastic analysis", Structures, 26, pp. 670–685, 2020. https://doi.org/10.1016/j.istruc.2020.03.065

[12] Heinisuo, M. "Axial resistance of double grade (S355, S420) hollow sections manufactured by SSAB", Design guides for high strength structural hollow sections manufactured by SSAB–for EN 1090 applications, 2014.

[13] Taras, A., Huemer, S. "On the influence of the load sequence on the structural reliability of steel members and frames", Structures, 4, pp. 91–104, 2015. https://doi.org/10.1016/j.istruc.2015.10.007

[14] Radwan, M., Kövesdi, B. "Equivalent local imperfections for FEM-based design of welded box sections", Journal of Constructional Steel Research, 199, 107636, 2022. https://doi.org/10.1016/j.jcsr.2022.107636

[15] Johansson, B., Maquoi, R., Sedlacek, G. "New design rules for plated structures in Eurocode 3", Journal of Constructional Steel Research, 57(3), pp. 279–311, 2001. https://doi.org/10.1016/S0143-974X(00)00020-1

[16] Kövesdi, B., Somodi, B. "Comparison of Safety Factor Evaluation Methods for Flexural Buckling of HSS Welded Box Section Columns", Structures, 15, pp. 43–55, 2018. https://doi.org/10.1016/j.istruc.2018.05.006

[17] Vrouwenvelder, T. "The JCSS probabilistic model code", Structural Safety, 19(3), pp. 245–251, 1997. https://doi.org/10.1016/S0167-4730(97)00008-8

[18] Afshan, S., Francis, P., Baddoo, N. R., Gardner, L. "Reliability analysis of structural stainless steel design provisions", Journal of Constructional Steel Research, 114, pp. 293–304, 2015. https://doi.org/10.1016/j.jcsr.2015.08.012

[19] Tuezney, S., Lauwens, K., Afshan, S., Rossi, B. "Buckling of stainless steel welded I-section columns", Engineering Structures, 236, 111815, 2021. https://doi.org/10.1016/j.engstruct.2020.111815

[20] ANSYS® "ANSYS Mechanical APDL, v18 2021", [computer program] Available at: https://www.ansys.com/

[21] Radwan, M., Kövesdi, B. "Improved design method for interaction buckling resistance of welded box-section columns", Journal of Constructional Steel Research, 194, 107334, 2022. https://doi.org/10.1016/j.jcsr.2022.107334

[22] Radwan, M., Kövesdi, B. "Enhanced buckling reduction factors using amplified imperfections for existing steel structures", Journal of Constructional Steel Research, 214, 108478, 2024. https://doi.org/10.1016/j.jcsr.2024.108478

[23] Radwan, M., Kövesdi, B. "Local plate buckling type imperfections for NSS and HSS welded box-section columns", Structures, 34, pp. 2628–2643, 2021. https://doi.org/10.1016/j.istruc.2021.09.011

[24] ECCS "European recommendations for steel construction; buckling of steel shells", European Convention for Constructional Steelwork, Brussels, 1988.

[25] European Committee for Standardization "prEN 1993-1-14:2020 Eurocode 3: Design of steel structures, Part 1-14: Design assisted by Finite element analysis (under development)", CEN, Brussels, Belgium, 2021.

[26] Pavlovčič, L., Froschmeier, B., Kuhlmann, U., Beg, D. "Finite element simulation of slender thin-walled box columns by implementing real initial conditions", Advances in Engineering Software, 44(1), pp. 63–74, 2012. https://doi.org/10.1016/j.advengsoft.2011.05.036

[27] Chan, H. U., Walport, F., Gardner, L. "Equivalent sway imperfections and sway-member imperfection combinations for GMNIA-based steel design", Structures, 62, 106216, 2024. https://doi.org/10.1016/j.istruc.2024.106216

[28] Liu, H., Shen, M., Hu, Y.-F., Chan, T.-M., Chung, K.-F. "Flexural buckling and design of press-braked rectangular hollow section steel long columns", Journal of Building Engineering, 109, 113004, 2025. https://doi.org/10.1016/j.jobe.2025.113004

[29] Sarquis, F. R., de Lima, L. R. O. "Numerical investigation of short-to-intermediate fixed-ended stainless steel bolted starred equal-leg angle columns", Journal of Constructional Steel Research, 215, 108557, 2024. https://doi.org/10.1016/j.jcsr.2024.108557

[30] Suman, S., Samanta, A., Singh, P. K. "Behaviour, design, and reliability of monosymmetric I-beams at elevated temperature", Structures, 63, 106342, 2024. https://doi.org/10.1016/j.istruc.2024.106342

[31] Lapira, L., Gardner, L., Wadee, M. A. "A new model for calculating the ultimate shear resistance of steel I-section girders", Thin-Walled Structures, 200, 111908, 2024. https://doi.org/10.1016/j.tws.2024.111908

[32] Zeng, Z., Ban, H., Shi, Y. "Local buckling behaviour of stainless-clad bimetallic steel cold-formed square hollow section stub columns", Thin-Walled Structures, 215, 113571, 2025. https://doi.org/10.1016/j.tws.2025.113571